$(\pi^{\pm},\pi^{\pm}p)$ reaction at 245 MeV

E. Piasetzky,* D. Ashery, A. Altman, and A. I. Yavin
Physics Department, Tel Aviv University, Tel Aviv, Israel

F. W. Schlepütz† and R. J. Powers‡
Physikinstitut der Universität Zürich, CH-8001 Zürich, Switzerland

W. Bertl, L. Felawka, and H. K. Walter
LHE der ETH Zürich, CH-5234 Villigen, Switzerland

R. G. Winter
Universität Zürich, Zürich, Switzerland
and College of William and Mary, Williamsburg, Virginia 23185

J. v. d. Pluym
Natuurkundig Laboratorium, Vrije Universiteit, Amsterdam, The Netherlands
(Received 30 July 1981)

The inclusive $(\pi^{\pm},\pi^{\pm}p)$ reactions on C, Fe, and Bi were studied at 245 MeV in a broad kinematic range by means of coincidence measurement of the outgoing particles. The π-p angular correlations and proton-energy spectra show features consistent with those expected from quasifree scattering. It is observed that about 80% of the inclusive inelastic scattering cross section at backward pion angles may be attributed to nucleon knockout mechanisms. The results allow identification of the direct quasifree process, unperturbed by higher order effects, which accounts for 30%, 20%, and 15% of the C, Fe, and Bi inclusive (π^{+},π^{+}) differential cross sections, respectively. The ratio of positive to negative pion cross sections for quasifree scattering, integrated over the proton energy and angle, are in agreement with the ratio for free π-p scattering. Such is not the case for various proton angles. The deviation of the positive to negative ratio at the peak of the proton angular correlation from the free scattering ratio is most pronounced for more forward pion angles.

[NUCLEAR REACTIONS $(\pi^{\pm},\pi^{\pm}p)$ coin. measurements on C, Fe, Bi, $E=245$ MeV; deduced σ_{knockout} decomposition of $\sigma_{\text{inelastic}}$.]

I. INTRODUCTION

A description of the pion-nucleus interaction depends strongly on the understanding of its reaction channels. This is important not only for the analysis of pion-induced reactions, but also for the interpretation of elastic scattering. The total reaction cross section was recently decomposed into the partial cross sections for the major reaction channels.[1] It was found that the cross section for true pion absorption (when there are no pions in the final state) is about equal to that for inelastic scattering (to all final states, excluding charge exchange), and that together they represent more than 80% of the total reaction cross section.

Studies of inclusive pion inelastic scattering[1,2] indicate that for scattering to the backward hemisphere the major reaction mechanism appears to be that of pion-nucleon quasifree scattering. This conclusion is based on the shape of the angular distribution of inelastically scattered pions which, for $\theta_{\pi} \geq 90°$, is similar to that of free pion-nucleon scattering.[1] The energy spectrum of the pions scattered to backward angles also has a shape which is consistent with that expected from quasifree scattering.[2] A similar situation is observed in electron scattering.[3] Since the pion mean free path is appreciably smaller than the diameter of nuclei, there is a

considerable probability for the scattered pion to undergo additional scattering on its way out. Such multiple scattering is virtually absent for electrons, but is dominant for protons and makes the observation of proton quasifree scattering very difficult.[4] For pions, the combination of kinematic conditions which allows quasifree scattering to backward angles (unlike the situation with protons), and true absorption, which suppresses the multiple scattering, makes it possible to observe quasifree scattering cleanly.

Much effort has been devoted in recent years to the search for pion-nucleus quasifree scattering. Several nucleon knockout experiments, studying the $^{12}C(\pi^{\pm},\pi N)^{11}C$ or $^{16}O(\pi^{\pm},\pi N)^{15}O$ reactions, used activation analysis[5] or prompt γ detection.[6] In these studies, the ratio of the observed cross section for positive and negative pions was calculated and compared to that expected from quasifree scattering. The failure of these experiments to reproduce the quasifree ratios was interpreted in various ways, and in particular, by suggesting that the outgoing nucleons undergo charge exchange in the final state interaction,[7,8] thereby modifying the cross-section ratio. By their nature, these experiments integrate over all the allowed phase space and are, therefore, not selectively sensitive to the quasifree process, which represents only part of the knockout reaction.

Experiments with more kinematic restrictions have been carried out with techniques such as: nuclear emulsions,[9,10] cloud chamber,[11] and bubble chamber.[12] In other experiments the outgoing particles were measured in coincidence.[13,14] While the former experiments cover a large part of the available phase space, they suffer from poor statistics. The coincidence measurements, on the other hand, had better statistics, but were confined to a narrow range of the available phase space. In a coincidence study of the $^{12}C(\pi^{\pm},\pi^{\pm}p)^{11}B$ reaction,[14] the population of low-lying states in ^{11}B was observed with a ratio consistent with the quasifree expectations, indicating that these transitions were in fact produced by quasifree scattering. The question of the role played by quasifree scattering in inclusive pion inelastic scattering and the contribution of pion multiple scattering remained open. Rough estimates of the multiple scattering contribution have been made,[15] but there has been no direct measurement of this effect.

The purpose of the present experiment was to study the $(\pi^{\pm},\pi^{\pm}p)$ reaction on several nuclei in a way that allows the separation of the quasifree scattering from higher order processes, and to provide the necessary information for the determination of the role of these processes in inclusive inelastic scattering. A part of the results presented in this work was published earlier.[16]

II. EXPERIMENTAL PROCEDURE

The experiment was done with the $\pi M3$ channel of the SIN accelerator at a bombarding energy of 245 MeV. For positive and negative incident pions, the outgoing protons and pions were detected in coincidence, and the energy spectra of the knocked-out protons were measured. Natural targets of C, Fe, and Bi of thicknesses 2, 2.5, and 4.5 g/cm^2, respectively, were used. The experimental setup is shown in Fig. 1. The pion beam hit the target after passing through two plastic scintillators, $P1$ and $P2$. The target was fitted into a 5×5-cm^2 hole in the center of a large plastic scintillator, $P4$. An anticoincidence with this collimating scintillator and a coincidence with the two scintillators $P1$ and $P2$ were required for beam monitoring and data acquisition. Protons present in the beam were eliminated by degraders positioned inside the beam transport channel. Muon and electron contaminations in the beam were measured by time of flight.

The scattered pions were detected by three telescopes, each consisting of two $5\times5\times5$-cm^3 cubes of plastic scintillator with 5-mm thick scintillators in front and back of the cubes (the back detector is not shown in the figure). The front surface of the telescopes was 50 cm from the target and their centers separated from each other by 10°.

Fast pions that passed through the front cube of a telescope were identified by the combination of their energy losses ($\Delta E1$,$\Delta E2$) in the two cubes. Particles that passed through both cubes were

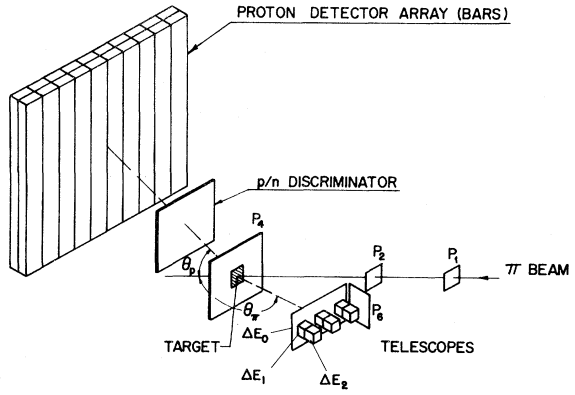

FIG. 1. The experimental setup (see text).

tagged by the scintillator positioned behind the telescopes. Slow pions that stopped in one of the front cubes were identified by the combination of their energy losses ($\Delta E0$,$\Delta E1$) in the front thin detector and in the cube. The energy-loss measurements, therefore, identified pions over the whole energy region. The pion-energy spectrum was not measured. The protons, in coincidence with pions in the telescopes, were detected with an array of twenty $5\times100\times10$ cm^3 plastic scintillator bars, arranged in two layers, and covering an area of 1 m^2. The front surface of the first layer was 111 cm from the target (Fig. 1). The proton-detector array could be moved so that the angular range of $-140°$ to 30° relative to the beam direction could be covered continuously, and cover simultaneously the vertical angular range from $-21°$ to 21°. A 1-mm thick scintillator was placed in front of the array to discriminate against neutrons. Pulse-height and time-of-flight information was recorded for each scintillator, with the time difference between pulses in the phototubes mounted at the ends of each scintillator giving the vertical position of the detected particle. The information was sufficient to identify protons and to measure their energy with moderate resolution.

Fast protons that passed through one of the front bars were identified by combining their energy losses in the front and back bars. Particles which stopped in one of the front bars were identified by their position in the energy versus time-of-flight spectrum. Particles heavier than protons (mainly deuterons) were also identified in this spectrum, as illustrated in Fig. 2, for the case of π^- on C.

Pions and protons from scattering on the hydrogen in a CH_2 target were detected in coincidence at several angles to provide proton-energy calibration. The overall energy resolution measured with the CH_2 target (including kinematic broadening, energy losses, and electronics) was 18 MeV in the measured proton energy range of 100–140 MeV. The resolution is expected to get worse with the decrease in proton energy. The proton angular resolution was 5°. The low energy cutoff for proton detection was 30 MeV.

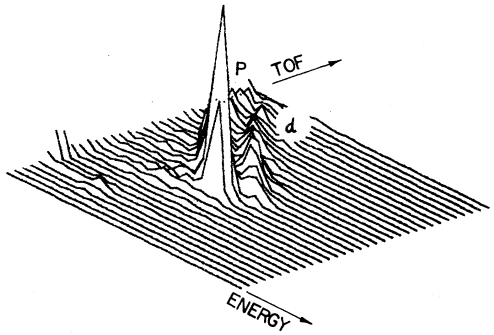

FIG. 2. A spectrum of energy vs time-of-flight for π^- on C.

For each of the investigated targets, pions were detected in the angular range of $70°-140°$ in steps of 10°, with an angular resolution of 5.2°. For each pion angle, protons were detected over an angular range of approximately 100°, centered around the angle for free pion-proton scattering.

For each position of the proton-detector array, the target angle was fixed so that the proton path in the target was minimized. Corrections were applied to account for the loss of pions and protons in the target due to secondary reactions as well as to the stopping of low energy pions and protons in the target and air. This latter correction is appreciable for the low energy end of the proton spectra, but hardly affects the angular correlations. The detection efficiency of the 1-mm thick detector (p/n detection in Fig. 1) was 98%. The combined muon and electron contamination was less than 0.5% for π^+ and 2% for π^-. All these corrections (bombarding energy, target, and angle dependence) were included in the absolute normalization. The absolute cross section was checked by measuring the free π-p cross section for several pion angles, and was found to agree, within the experimental uncertainty, with previously measured values.[17]

III. RESULTS AND DISCUSSION

A three-dimensional display of the pion-proton angular correlation, integrated over the particle energies, is shown in Fig. 3. The pions were detected at a fixed angle $\theta_\pi=140°$, while the protons were detected in the angular region of $-125°\leq\theta_p\leq5°$ for π^+ and $-105°\leq\theta_p\leq0°$ for π^- in the reaction plane, and at $-21°\leq\varphi_p\leq21°$ in the perpendicular plane. A strong peak is observed at an angle corresponding to the kinematic conditions for free π-p scattering. In Fig. 4, we show a slice of this correlation along the reaction plane, with a width $\Delta\varphi_p=\pm6°$, for C, Fe, and Bi. The errors shown contain statistical and angle dependent systematic uncertainties. There is an additional overall normalization uncertainty of $\pm8\%$. The scale of the π^- cross section for C is that for π^+ scattering multiplied by the π^-p/π^+p ratio of cross sections for free π-p scattering.[17]

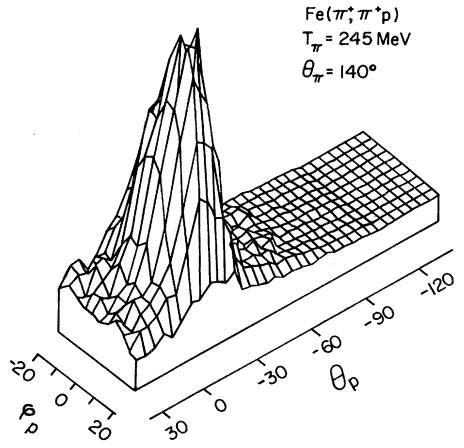

FIG. 3. A three dimensional display of pion-proton angular correlation.

These curves and those obtained for all the other pion-scattering angles show strong peaks centered near the angles corresponding to the kinematic condition for free pion-nucleon scattering, superimposed on a low "background." Proton-energy spectra, in coincidence with π^+ and π^- measured at the peak of the angular correlation curves, are shown in Fig. 5(a). Again we observe a peak centered near the energy corresponding to free π-p scattering. The width of the peak, adjusted for experimental energy resolution, is (37 ± 3) MeV for π^+ scattering and (50 ± 10) MeV for π^- scattering (FWHM). Energy spectra at angles away from the angular correlation peak are shown in Fig. 5(b) and are somewhat shifted in peak position and somewhat broader, but always fall off to very low values well above the experimental cutoff energy. We can therefore conclude that the shape of the angular correlation is not appreciably affected by this cutoff.

The pion-proton angular correlations were fitted by a least square method to a sum of two Gaussians with peak positions, amplitudes, and widths treated as free parameters. The solid curves in Fig. 4 show the results of the fit. We obtain for all cases one narrow and one broad Gaussian. The width of the narrow Gaussian varies only slightly from one target nucleus to another (see Table I); the broad Gaussian is 2—3 times wider. The peak of the narrow Gaussian lies near the angle corresponding to free π-p scattering. For positive pions, the standard deviation of the narrow Gaussian is approximately equal to $0.45\times\tan^{-1}[p_F/p_p(\theta_\pi)]$, where p_F is the Fermi momentum of a proton in the target nucleus and $p_p(\theta_\pi)$ is the momentum of a proton scattered in free π-p collision when the pion is detected at θ_π.

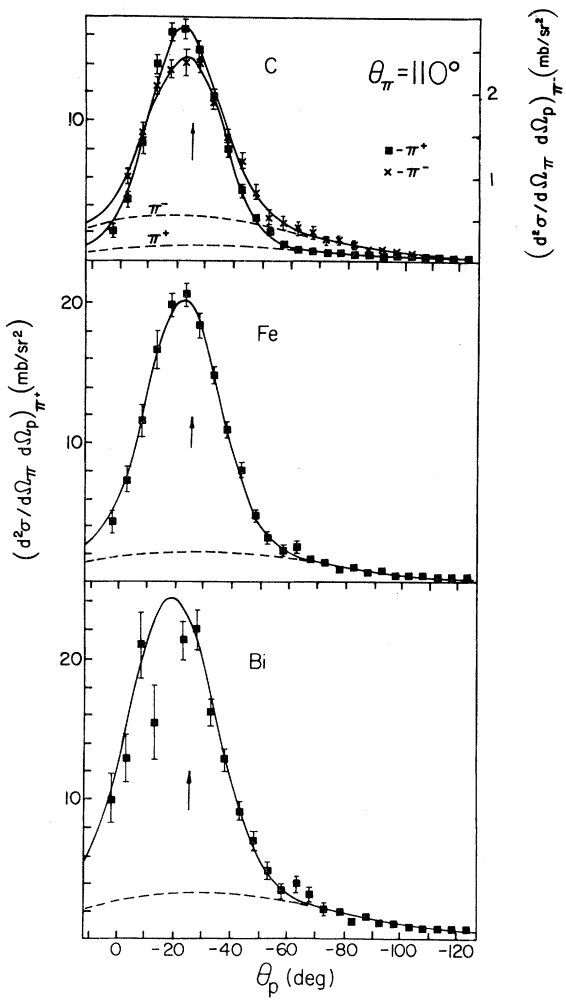

FIG. 4. Slices of the angular correlation along the reaction plane with width $\Delta\varphi_p = \pm 6°$ for C, Fe, and Bi for π^+ (squares) and π^- (crosses). Each solid curve is the result of a two-Gaussian fit to the data. The arrow marks the angle for free π-p scattering. The dashed curves are the broad Gaussians.

We would like to emphasize that the equation describes quantitatively the narrow-Gaussian widths but only qualitatively the connection with the Fermi motion. p_F is the Fermi momentum at the center of the nucleus while it should be evaluated at the point of interaction, near the surface of the nucleus. Moreover, kinematic restriction to a plane should reduce the width by a $\sqrt{2/3}$ factor. The broad Gaussian (shown by dashed curves in Fig. 4) has a standard deviation of about 40° for all the measured angular correlations. As can be observed in Fig. 4, the angular correlation for π^- scattering is broader than than for π^+ scattering. These results indicate

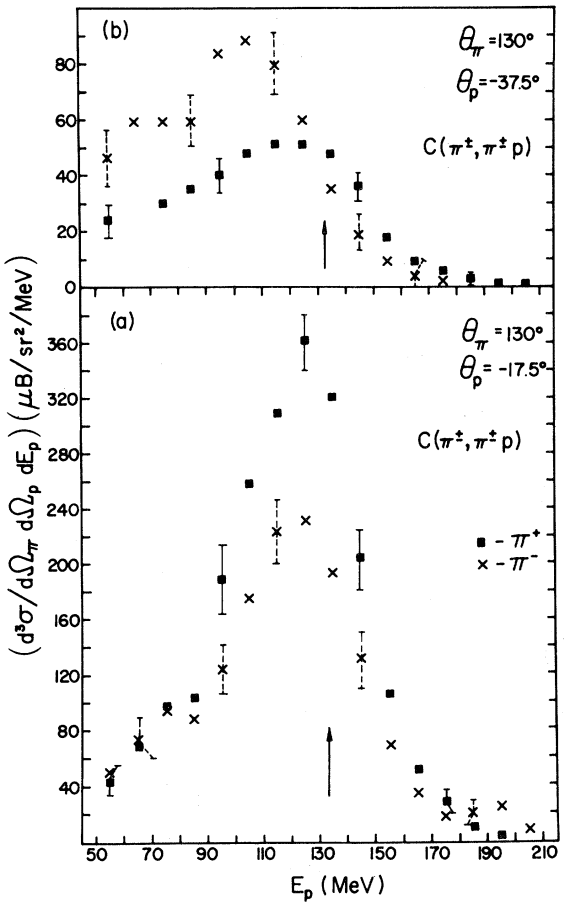

FIG. 5. Proton-energy spectra measured on C (a) at the peak of the angular correlation and (b) off this peak. The arrow marks the energy for free π-p scattering.

that we may associate the narrow Gaussian of the angular correlation with quasifree pion-proton scattering, while the broad Gaussian represents the effects of pion multiple scattering and nucleon final state interactions. The relative contribution from pion multiple scattering is expected to be similar for π^+ and π^-. For π^- there exists the strong additional channel (π^-,π^-n) which will become observable if the n undergoes charge exchange; compared with this the (π^+,π^+n) reaction followed by charge exchange will be negligible. In Tables I and II we present the parameters of the narrow Gaussian. These are the amplitude, the peak angle, and the standard deviation. Also shown is the angle for free π-p scattering. The error in the amplitude is that of the absolute normalization (8%), the errors in the peak position and standard deviation are about $\pm 1°$. The errors from the fitting procedure are small compared to these values.

While the fits discussed above were made for the data in the reaction plane, we note that the data outside the reaction plane have a very similar shape. In Fig. 6 we show a cut through the data in the plane perpendicular to the reaction plane together with the data and the fit done for the reaction plane. The result indicates that the spatial distribution of the quasifree peak is symmetric in all dimensions about its center.

The role of the (π^+,π^+p) reaction in the inclusive (π^+,π^+) reaction can be seen in several ways. We first discuss the contribution from the narrow Gaussian, which we regard as representing the one step quasifree scattering, unperturbed by nucleon final state interactions or by any other higher order incoherent effect. Integration of the double differential cross section over this Gaussian gives the quasifree differential cross section, $d\sigma/d\Omega_{\pi qf}$ (θ_π) which is the contribution of this process to the inclusive differential cross section[1] for (π^+,π^+). In performing the integration we used the fact that the quasifree peak was observed to have the same shape in and out of the reaction plane. The results of this integration are shown in Table I. These values are also plotted in Fig. 7, where the lines are the cross sections for free π-p scattering scaled to the data by a factor of 0.9, 1.36, and 1.89 for C, Fe, and Bi, respectively. These numbers increase with A more slowly than the values of N_{eff},[1] which represent a similar scaling done to the inclusive inelastic scattering. This behavior can be understood as resulting from losses due to nucleon final state interaction, which increase with atomic weight A.

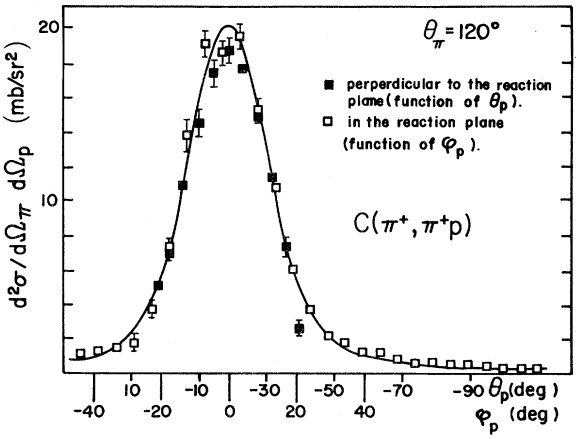

FIG. 6. A $\pm 6°$ slice of the C (π^+,π^+p) angular correlation in the plane perpendicular to the reaction plane together with a similar slice in the reaction plane. The solid curve is the result of a two-Gaussian fit to the data in the reaction plane.

TABLE I. Parameters of the narrow (quasifree) Gaussian, the angle for free π-p scattering, the integral of the double differential cross section over the quasifree Gaussian ($d\sigma/d\Omega_{\pi^+}$ qf), the integral of the double differential (π^+,π^+p) cross section over all space [$\sigma(\pi^+,\pi^+p)$], and the cross section for (π^+,π^+), for 245 MeV π^+.

	Parameters of the quasifree Gaussian							
Target	Pion angle ($\theta\pi$)	Amplitude (mb/sr^2)	Stand. dev.	Peak angle	Free proton angle	$d\sigma/d\Omega_\pi$qf (mb/sr)	$d\sigma/d\Omega$ ($\pi,\pi p$) (mb/sr)	$d\sigma/d\Omega$ (π^+,π^+)[a] (mb/sr)
C	70°	6.0	13.9°	41°	45.2°	2.2±0.4	6.4±0.8	13.4±1.1
	90°	9.5	13.4°	30.4°	35.0°	3.3±0.6	6.1±0.7	11.7±0.9
	100°	12.35	12.5°	25.8°	30.4°	3.7±0.7	7.7±0.9	13.4±1.1
	110°	15.7	12.3°	22.1°	26.1°	4.6±0.8	7.8±0.9	14.4±1.1
	120°	18.4	11.0°	19.2°	21.9°	4.3±0.8	8.7±1.0	14.5±1.2
	130°	20.9	10.9°	16.0°	18.0°	4.8±0.9	9.1±1.1	17.5±1.4
	140°	22.1	10.7°	12.6°	14.2°	4.9±0.9	9.5±1.1	17.7±1.4
Fe	70°	6.6	17.5°	39.5°	45.2°	3.9±0.7	10.8±1.3	23.5±1.9
	90°	9.9	15.4°	30.5°	35.0°	4.5±0.8	12.8±1.5	24.4±2.0
	100°	13.5	13.6°	25.6°	30.4°	4.8±0.9	14.3±1.7	25.1±2.0
	110°	17.9	13.3°	22.0°	26.1°	6.1±1.1	13.9±1.7	29.9±2.4
	120°	21.2	13.2°	18.0°	21.9°	7.0±13	15.0±1.8	30.4±2.4
	130°	24.7	12.3°	15.2°	18.0°	7.1±1.3	17.0±2.0	35.2±2.8
	140°	28.4	12.4°	12.5°	14.2°	8.3±1.5	17.6±2.1	40.4±3.2
Bi	70°	7.2	20.2°	33.2°	45.2	5.6±1.0	12.5±1.5	45.1±3.6
	90°	10.5	18.2°	26.7°	35.0	6.6±1.2	15.9±1.9	49.9±4.0
	100°	15.4	16.2°	23.0°	30.4	7.7±1.4	19.1±2.3	52.6±4.2
	110°	21.2	15.2°	18.5°	26.1	9.4±1.7	22.8±2.7	56.0±4.5
	120°	22.0	14.6°	16.3°	21.9	9.0±1.6	37.2±4.5	54.8±4.4
	130°	27.0	13.3°	13.4°	18.0	9.1±1.6	25.6±3.1	71.8±5.7

[a]Measured data of Ref. 1

The ratio of the $d\sigma/d\Omega_{\pi qf}$ (θ_π) values for π^+ and π^- is shown in Fig. 8(a) together with the ratio for free $\pi^\pm$-p scattering. As can be seen, the agreement is good. We must note, however, that while the ratio of the integral over the proton angles is in agreement with the ratio for free π-p scattering, such is not the case for certain proton angles, as can be seen from Fig. 4. The deviation of the ratio at the peak of the angular correlation ranges from 90% at $\theta_\pi=90°$ to 15% at $\theta_\pi=140°$, as can be seen in Fig.

TABLE II. Same as Table I, but for π^-.

	Parameters of the quasifree Gaussian							
Target	Pion angle ($\theta\pi$)	Amplitude (mb/sr^2)	Stand. dev.	Peak angle	Free proton angle	$d\sigma/d\Omega_\pi$qf (mb/sr)	$d\sigma/d\Omega$ ($\pi,\pi p$) (mb/sr)	$d\sigma/d\Omega$ (π^-,π^-)[a] (mb/sr)
C	70°	0.66	20.0°	43.2°	45.2°	0.50±0.1	1.38±0.16	13.4±1.1
	90°	0.92	16.0°	31.5°	35.0°	0.45±0.08	1.78±0.2	11.7±0.9
	100°	1.37	14.0°	26.9°	30.4°	0.51±0.1	1.96±0.23	13.4±1.1
	110°	1.95	13.7°	22.6°	26.1°	0.71±0.13	2.48±0.3	14.4±1.1
	120°	2.47	14.1°	19.8°	21.9°	0.95±0.17	3.31±0.4	14.5±1.2
	130°	3.01	13.7°	16.0°	18.0°	1.08±0.2	3.33±0.4	17.5±1.4
	140°	2.99	12.2°	13.6°	14.2°	0.8±0.15	3.27±0.4	17.7±1.4

[a]Assumed equal to $d\sigma/d\Omega(\pi^+,\pi^+)$.

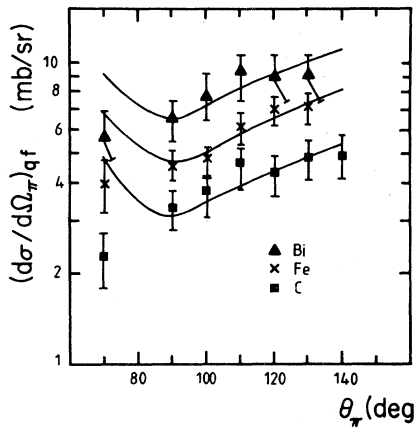

FIG. 7. The angular distribution of the quasifree (π^+,π^+p) cross section for C, Fe, and Bi. The lines are the cross sections for free π-p scattering scaled to the data.

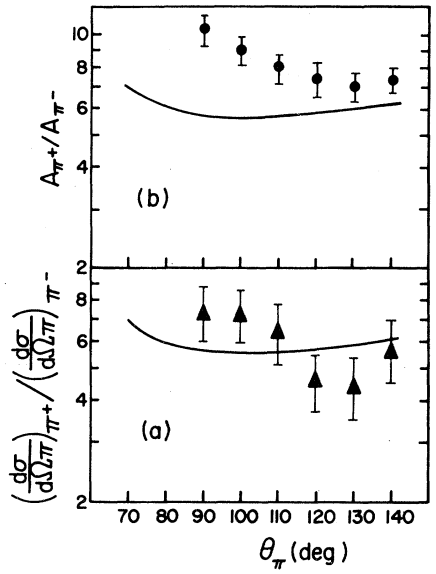

FIG. 8. (a) Ratios of the quasifree differential cross section $d\sigma/d\Omega_{\pi qf}$ for π^+ and π^- on C as a function of the pion angle. The line is the free π^+p to π-p cross section ratio. (b) The ratio of the quasifree double differential cross section $d^2\sigma/d\Omega_\pi d\Omega_p = A$ at the peak of the π-p angular correlations for π^+ and π^-.

8. An interpretation of this deviation in terms of destructive interference effects was proposed by Lenz and Moniz.[18] As can be seen from Table I, the quasifree process accounts for approximately 30%, 20%, and 15%, for C, Fe, and Bi, respectively, of the inclusive inelastic scattering cross section.

An alternative way to determine the role of the $(\pi,\pi p)$ process is to include all the data under the broad Gaussian which presumably also originate from a quasifree $(\pi,\pi p)$ process, and are perturbed by second order effects. This evaluation is done by integrating the two Gaussians over all space to get $\sigma(\pi,\pi p)$. The results are reported in Table I. We note that the ratio $(d\sigma/d\Omega)_{qf}/(d\sigma/d\Omega)_{\pi\pi p}$ is quite constant, for a given target, supporting the assumption that both originate from the same process. The integration procedure is based on the assumption that we may extrapolate the Gaussian fit beyond the region where data are available. In justifying this extrapolation we first note that while the measurements in the reaction plane extended over more than 100°, they cover only 42° in the perpendicular plane. However, over this region the angular distributions in both planes have the same shape. While this similarity may not be *a priori* obvious for $|\theta_p|$ and $|\varphi_p| \leq 21°$, there is no reason to expect the two shapes to be different as we go farther away from the peak. In fact, we may expect that higher order effects, like multiple scattering, will be even more isotropic. In order to get a measure of the precision of the procedure, we integrated the data over the measured part of the space and calculated the integration over the same part by using the fitted Gaussians. The results differ by less than 5%. In addition, integration over the measured space accounts for more than 70% of the integration over all space. Assuming a larger error for the extrapolated part will, therefore, not affect the results appreciably. In quoting errors for this integral we assumed that the uncertainty in the extrapolated region is twice that in the measured region.

When comparing the resulting differential $(\pi,\pi p)$ cross sections to the inclusive (π,π') cross sections, we find that $(\pi,\pi p)$ accounts for about 55%, 50%, and 40% for C, Fe, and Bi, respectively. The missing part of the cross sections can be attributed to the following processes.

A. Deuteron emission

Deuteron emission was observed by identifying the deuterons in the time of flight versus energy spectra (see Fig. 2). Each pion-deuteron angular correlation shows a peak similar to that observed in the pion-proton correlation. This result may be consistent with a direct deuteron knockout as well

as with a coherent pickup mechanism. The deuteron yield is about 4% of the total (π^+,π^+p) yield discussed above, and therefore represents only about 2% of the (π^+,π^+) cross section. In the π^- measurement the deuteron yield is 12% of the (π^-,π^-p) yield. The cross sections for deuteron emission may be larger, since the deuteron's energy is lower and the energy loss in the target and air is larger than that for protons, so that part of the yield may be below the detection threshold. Other heavy clusters, such as α particles, might also be ejected but could not be detected. The deuteron yield is approximately the same for π^+ and π^- measurements on carbon.

B. Neutron emission

For carbon, we may assume that the (π^+,π^+n) contribution, from both a direct process and a $\pi^+,\pi^+p)$ reaction followed by nucleon charge exchange, is equal to the (π^-,π^-p) contribution. This accounts for about 20% of the (π,π') cross section. For the heavier targets both effects are larger and it may reach 25% and 30% for Fe and Bi, respectively.

When we add the contributions from these processes, we find that about 80% of the inelastic pion cross section may be attributed to nucleon knockout reactions. This fact confirms that this mechanism indeed dominates inelastic scattering.

IV. CONCLUSION

This work presents the results of a systematic study of the $(\pi,\pi p)$ reaction at 245 MeV over a broad kinematic range. The results allow identification of the direct quasifree process, unperturbed by higher order effects. The effects of quasifree scattering are most pronounced in light nuclei and at backward pion scattering angles, and decrease for more forward pion angles and heavier nuclei. It is observed that about 80% of the inelastic scattering cross section may be attributed to nucleon knockout mechanisms. This study of the angular and mass dependence of the quasifree scattering contribution leads to a better understanding of the $(\pi,\pi p)$ reaction mechanism.

ACKNOWLEDGMENTS

We thank Professor C. Joseph for allowing us to use the detector array, Dr. P. Shrager for his assistance in its operation, and Dr. I. Navon for his help in the preliminary stages of the experiment. Illuminating discussions with Prof. J. M. Eisenberg, Prof. J. Alster, and Prof. Z. Fraenkel, and Dr. F. Lenz, Dr. E. Moniz, Dr. E. Levin, and Dr. J. Lichtenstadt are gratefully acknowledged. The Tel Aviv University group is grateful for the warm hospitality of the Schweizerisches Institut für Nuklearforschung. This work was supported in part by the Israeli Commission for Basic Research and by the Swiss Institute for Nuclear Research.

---

*Present address: LAMPF, Los Alamos, New Mexico 87545.

†Present address: Schweizerisches Institut für Nuklearforschung, CH-5234 Villigen, Switzerland.

‡Present address: California Institute of Technology, Pasadena, California.

[1]D. Ashery *et al.*, Phys. Rev. C 23, 2173 (1981).

[2]C. H. Q. Ingram, in *Meson-Nuclear Physics — 1979 (Houston),* Proceedings of the 2nd International Topical Conference on Meson-Nuclear Physics, edited by E. V. Hungerford III (AIP, New York, 1979), p. 455.

[3]E. J. Moniz *et al.*, Phys. Rev. Lett. 26, 445 (1971).

[4]I. Tanihata *et al.*, Phys. Lett. 97B, 363 (1980).

[5]B. J. Dropesky *et al.*, Phys. Rev. C 20, 1844 (1979).

[6]C. L. Morris *et al.*, Phys. Rev. C 17, 227 (1978).

[7]P. W. Hewson, Nucl. Phys. A133, 659 (1969).

[8]M. M. Sternheim and R. R. Silbar, Phys. Rev. C 21, 1974 (1980).

[9]Yu. R. Gismatullin *et al.*, Yad. Fiz. 11, 285 (1970) [Sov. J. Nucl. Phys. 11, 159 (1970)]; Yad. Fiz. 19, 45 (1974) [Sov. J. Nucl. Phys. 19, 22 (1974)]; Yad. Fiz. 21, 950 (1975) [Sov. J. Nucl. Phys. 21, 488 (1975)].

[10]Ya. A. Berdnikov *et al.*, Yad. Fiz. 25, 938 (1977) [Sov. J. Nucl. Phys. 25, 499 (1977)]; Yad. Fiz. 25, 1150 (1976) [Sov. J. Nucl. Phys. 25, 610 (1977)].

[11]F. Balestra *et al.*, Nucl. Phys. A340, 372 (1980).

[12]E. Bellotti *et al.*, Nuovo Cimento 14A, 567 (1973).

[13]L. W. Swenson *et al.*, Phys. Rev. Lett. 40, 10 (1978).

[14]H. J. Ziock *et al.*, Phys. Rev. Lett. 43, 1919 (1979).

[15]D. Ashery, *Proceedings of the 8th Conference on High Energy and Nuclear Structure, Vancouver,* edited by D. F. Measday and A. W. Thomas (North-Holland, Amsterdam, 1979), p. 385.

[16]E. Piasetzky *et al.*, Phys. Rev. Lett. 46, 1271 (1981).

[17]P. J. Bussey *et al.*, Nucl. Phys. B58, 363 (1973).

[18]F. Lenz and E. Moniz, private communication.